Research Article | Vol. 24, No. 23 | 14 Nov 2016 | OPTICS EXPRESS 27009

Optics EXPRESS

Holographic tracking and sizing of optically trapped microprobes in diamond anvil cells

F. Saglimbeni,[1,*] S. Bianchi,[1] G. Gibson,[2] R. Bowman,[3] M. Padgett,[2] and R. Di Leonardo[1,4]

[1]*CNR-NANOTEC, Soft and Living Matter Laboratory, I-00185 Roma, Italy*
[2]*School of Physics and Astronomy, University of Glasgow, Glasgow G12 8QQ, UK*
[3]*NanoPhotonics Centre, Cavendish Laboratory, Department of Physics, University of Cambridge, JJ Thomson Avenue, Cambridge, CB3 0HE, UK*
[4]*Dipartimento di Fisica, Università di Roma "Sapienza", I-00185, Roma, Italy*
[*]*filippo.saglimbeni@roma1.infn.it*

Abstract: We demonstrate that Digital Holographic Microscopy can be used for accurate 3D tracking and sizing of a colloidal probe trapped in a diamond anvil cell (DAC). Polystyrene beads were optically trapped in water up to Gigapascal pressures while simultaneously recording in-line holograms at 1 KHz frame rate. Using Lorenz-Mie scattering theory to fit interference patterns, we detected a 10% shrinking in the bead's radius due to the high applied pressure. Accurate bead sizing is crucial for obtaining reliable viscosity measurements and provides a convenient optical tool for the determination of the bulk modulus of probe material. Our technique may provide a new method for pressure measurements inside a DAC.

© 2016 Optical Society of America

OCIS codes: (170.0180) Microscopy; (090.1995) Digital holography; (290.4020) Mie theory; (350.4855) Optical tweezers or optical manipulation.

References and links

1. S. H. Lee, Y. Roichman, G. R. Yi, S. H. Kim, S. M. Yang, A. van Blaaderen, P. van Oostrum, and D. G. Grier, "Characterizing and tracking single colloidal particles with video holographic microscopy," Opt. Express **15**, 18275–18282 (2007).
2. G. Bolognesi, S. Bianchi, and R. Di Leonardo, "Digital holographic tracking of microprobes for multipoint viscosity measurements," Opt. Express **19**, 19245–19254 (2011).
3. A. Ashkin, J. M. Dziedzic, J. E. Bjorkholm, and S. Chu, "Observation of a single-beam gradient force optical trap for dielectric particles," Opt. Lett. **11**, 288–290 (1986).
4. J. E. Curtis, B. A. Koss, and D. G. Grier, "Dynamic holographic optical tweezers," Opt. Commun. **207**, 1–6 (2002).
5. G. M. Gibson, R. W. Bowman, A. Linnenberger, M. Dienerowitz, D. B. Phillips, D. M. Carberry, M. J. Miles, and M. J. Padgett, "A compact holographic optical tweezers instrument," Rev. Sci. Instrum. **83**, 113107 (2012).
6. S. Keen, A. Yao, J. Leach, R. Di Leonardo, C. Saunter, G. Love, J. Cooperd, and M. Padgett, "Multipoint viscosity measurements in microfluidic channels using optical tweezers," Lab Chip **9**, 2059–2062 (2009).
7. G. Pesce, G. Rusciano, and A. Sasso, "Blinking Optical Tweezers for microrheology measurements of weak elasticity complex fluids," Opt. Express **18**, 2116–2126 (2010).
8. Q. L., T. Asavei, T. Lee, H. Rubinsztein-Dunlop, S. He, and I. I. Smalyukh, "Measurement of viscosity of lyotropic liquid crystals by means of rotating laser-trapped microparticles," Opt. Express **19**, 25134–25143 (2011).
9. M. Pitzek, R. Stieger, G. Thalhammer, S. Bernet, and M. Ritsch-Marte, "Optical mirror trap with a large field of view," Opt. Express **17**, 19414–19423 (2009).
10. S. Zwick, T. Haist, Y. Miyamoto, L. He, M. Warber, A. Hermerschmidt, and W. Osten, "Holographic twin traps," J. Opt. A **11**, 03011 (2009).
11. A. Jayaraman, "Diamond anvil cell and high-pressure physical investigations," Rev. Mod. Phys. **55**, 65–108 (1983).
12. R. W. Bowman, G. M. Gibson, M. J. Padgett, F. Saglimbeni, and R. Di Leonardo, "Optical trapping at gigapascal pressures," Phys. Rev. Lett. **110**, 095902 (2013).
13. R. W. Bowman, F. Saglimbeni, G. M. Gibson, R. Di Leonardo, and M. J. Padgett, "Optical tweezing at extremes," in *Optical Trapping and Optical Micromanipulation X*, Proc. SPIE **8810**, 881009, K. Dholakia and G. C. Spalding (SPIE, 2013).
14. R. R. Brau, J. M. Ferrer, H. Lee, C. E. Castro, B. K. Tam, P. B. Tarsa, P. Matsudaira, M. C. Boyce, R. D. Kamm, and M. J. Lang, "Passive and active microrheology with optical tweezers," J. Opt. A **9**, S103–S112 (2007).
15. F. J. MartÃηnez Boza and C. Gallegos, *Rheology-Volume I* (EOLSS Publications, 2010).
16. H. W. Moyses, B. J. Krishnatreya, and D. G. Grier, "Robustness of Lorenz-Mie microscopy against defects in illumination," Opt. Express **21**, 5968–5973 (2013).

#275140 http://dx.doi.org/10.1364/OE.24.027009
Journal © 2016 Received 7 Sep 2016; revised 13 Oct 2016; accepted 13 Oct 2016; published 11 Nov 2016

Optics EXPRESS

17. C. Bohren and D. Huffman, *Absorption and Scattering of Light by Small Particles* (Wiley Interscience, 1983).
18. A. Dewaele, J. H. Eggert, P. Loubeyre, and R. Le Toullec, "Measurement of refractive index and equation of state in dense He, H_2, H_2O, and Ne under high pressure in a diamond anvil cell," Phys. Rev. B **67**, 094112 (2003).
19. F. Saglimbeni, S. Bianchi, G. Bolognesi, G. Paradossi, and R. Di Leonardo, "Optical characterization of an individual polymer-shelled microbubble structure via digital holography," Soft Matter **8**, 8822–8825 (2012).
20. S. Bianchi and R. Di Leonardo, "Real-time optical micro-manipulation using optimized holograms generated on the GPU," Comp. Phys. Comm. **181**, 1444–1448 (2010).
21. B. M. Hanser, M. G. L. Gustafsson, D. A. Agard, and J. W. Sedat, "Phase-retrieved pupil functions in wide-field fluorescence microscopy," J. Microsc. **216**, 32–48 (2004).
22. P. de Groot and X. Colonna de Lega, "Interpreting interferometric height measurements using the instrument transfer function," in *Fringe 2005: the 5th International Workshop on Automatic Processing of Fringe Patterns*, W. Osten, eds. (Springer, 2006), pp. 30–37.
23. R. A. Forman, G. J. Piermarini, J. D. Barnett, and S. Block, "Pressure measurement made by the utilization of ruby sharp-line luminescence," Science **176**, 284–285 (1972).
24. A. D. Chijioke, W. J. Nellis, A. Soldatov, and I. F. Silvera, "The ruby pressure standard to 150 GPa," J. Appl. Phys. 98, 114905 (2005).
25. K. Berg-Sørensen and H. Flyvbjerg, "Power spectrum analysis for optical tweezers," Rev. Sci. Instrum. **75**, 594 (2004).
26. E. H. Abramson, "Viscosity of water measured to pressures of 6 GPa and temperatures of 300°," Phys. Rev. E **76**, 051203 (2007).
27. K. E. Bett and J. B. Cappi, "Effect of pressure on the viscosity of water," Nature **207**, 620–621 (1965).
28. E. J. G. Peterman, F. Gittes, and C. F. Schmidt, "Laser-induced heating in optical traps," Biophys J. **84**, 1308–1316 (2003).
29. http://webbook.nist.gov/chemistry/fluid/
30. R. Kono, "The dynamic bulk viscosity of polystyrene and polymethyl methacrylate," J. Phys. Soc. Jpn. **15**, 718–725 (1960).
31. P. H. Mott, J. R. Dorgan, and C. M. Roland, "The bulk modulus and Poisson's ratio of "incompressible" materials," J. Sound. Vib. **312**, 572–575 (2008).
32. T. Kenichi, "Bulk modulus of osmium: high-pressure powder x-ray diffraction experiments under quasihydrostatic conditions," Phys. Rev. B **70**, 012101 (2004).
33. J. R. Hemley, P. M. Bell, and H. K. Mao, "Laser techniques in high-pressure geophysics," Science **237**, 605–612 (1987).

1. Introduction

Digital holographic microscopy (DHM) can be used in combination with Mie scattering theory to simultaneously track and characterize colloidal particles with nanometer resolution [1]. The possibility of precisely sizing a colloidal probe particle is crucial for retrieving absolute viscosity measurements from the center of mass dynamics of the probe bead [2]. Holographic optical tweezers (HOT) [3–5] offer a powerful tool for microrheological studies [6–8] and, when combined with DHM, allow for a full 3D and multipoint particle tracking for viscosity measurements [2]. The need for a high numerical aperture for stable axial trapping has confined HOT to situations where samples could be accessed using short working distance objectives. Using a mirror trap configuration [9, 10] and a diamond anvil cell (DAC) [11] we have recently shown that the full power of holographic tweezers can be also made available for high pressure studies [12, 13]. Optical tweezers have been successfully applied to the study of the mechanical and rheological response of soft and biological matter [14]. Although high applied pressures are known to produce dramatic structural changes in soft materials, the study of the corresponding changes in dynamical properties is still largely unexplored. Moreover, in contrast to other existing techniques for high pressure rheology [15], our method gives direct access to absolute viscosity measurements at gigapascal pressures. In our previous work [12], a trapped bead was used as a micron-sized probe for absolute viscosity measurements under high pressures up to crystallization (2 GPa). The technique requires the a priori knowledge of the probe's diameter which is usually provided by the manufacturer with a standard deviation ranging from 3% to 15%. This fact prevents accurate viscosity measurements leading to systematic errors of the order of a few percent.

In the present work we combine the holographic counter-propagating optical trap setup with

Optics EXPRESS

in-line Digital Holographic Microscopy. A coherent light beam is scattered by a spherical probe particle producing a fringe pattern magnified by a microscope. Fitting this interference pattern to Lorenz-Mie scattering theory we can recover the 3D position of the bead, its refractive index, and its radius [1, 2]. The analysis of the Brownian particle fluctuations, together with a high precision sizing, allows for accurate and absolute viscosity measurements in highly pressurized samples. The high sensitivity of Mie scattering to probe radius can be further used to monitor pressure induced size changes. This allowed us to obtain an unreported measurement of pressure dependent bulk modulus of colloidal polystyrene bead up to 2 GPa.

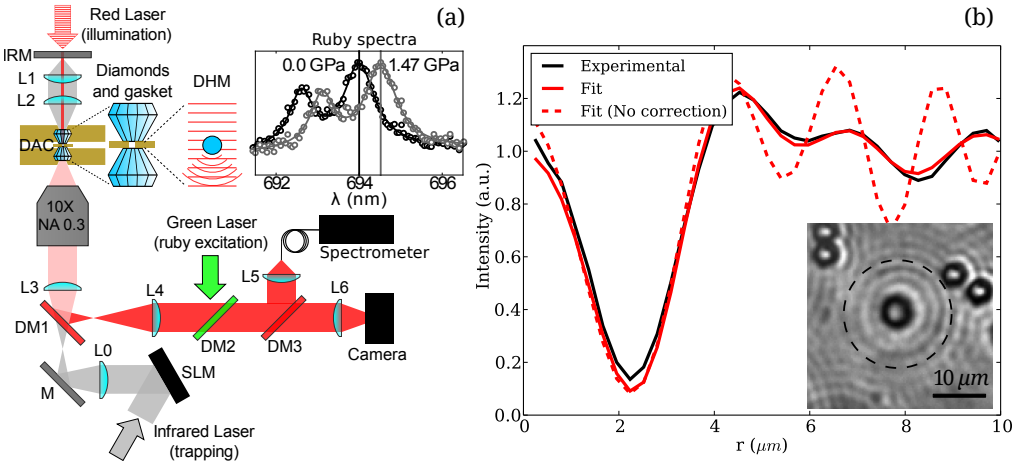

Fig. 1. (a) Schematic view of the optical setup. L1, L2, L3, L4, L5, L6, lenses; IRM infrared mirror; DM1, DM2, DM3 dichroic mirrors; M mirror. (b) Radial histogram (black line) of the experimentally recorded hologram (shown in the inset) with fit (red line). The red dashed line is obtained without taking into account the limited NA and the aberration due to the diamond window (see text). Black dashed line in the inset delimits the region where the hologram is fitted.

2. Methods

A DAC is essentially composed by two diamond anvils held in a metallic structure that can push them against each other. The diamonds are kept separated by a metallic gasket with a hole (200 μm diameter, 50 μm height) in which the sample is placed. Our DAC (EasyLab, μScope DAC-RT(G)) has a working distance to sample of 8 mm while its NA is 0.54. Consequently, we use a 10X objective with 12 mm working distance and 0.3 NA. Stable 3D trapping is impossible at such a low NA when using a single trapping beam. To overcome this problem, we have modified our portable holographic optical tweezers instrument [5] (see Fig. 1(a)) to produce two counter propagating beams [12, 13]. A Spatial Light Modulator (Boulder P512-1064) splits the laser (IPG YLM-5-LP-SC, λ = 1070 nm) in a collimated and a divergent beam. While the collimated beam is focused on the objective focal plane, the divergent one focuses 300 μm above and thus exerts a negligible radiation pressure. However, the divergent beam is collected by the lenses L1-L2 and reflected back by an IR mirror (see Fig. 1(a)). After being reflected, this counter propagating beam focuses again in the sample in a spot placed a few microns above the focal plane. Therefore, we have two counter-propagating beams, which are focused into two nearby spots aligned along the vertical axis, resulting in a 3D stable trap.

The sample is illuminated by a red laser diode (λ = 640 nm). If the incident beam divergence angle is $\lesssim$ 1 mrad, the illumination can be treated as a linearly polarized plane wave [16]. In this

Optics EXPRESS

situation the field scattered by a spherical particle is predicted exactly by Mie theory [17]. The corresponding intensity pattern (the *hologram*) is:

$$I = |1 + \mathbf{f}(\mathbf{r} - \mathbf{r}_p, a, n_p, n_w)|^2 |E_i|^2 \tag{1}$$

where E_i is the amplitude of the incident plane wave, $\mathbf{f}$ is an analytically known function of particle position $\mathbf{r}_p = (x_p, y_p, z_p)$, radius a, particle and medium refractive indexes n_p and n_w. The hologram, normalized in order to eliminate the dependence from E_i, can be fitted using a Levenberg-Marquardt nonlinear least-squares minimization algorithm with the five free parameters: x_p, y_p, z_p, a, n_p. Since our particles are dispersed in water, instead of fitting n_w, we use the values in [18] for water refractive index as a function of pressure. The fitting procedure requires the calculation of a few hundreds holograms of 124×124 pixels, thus we exploited the computational power of a CUDA based graphic processing unit (GTX-470) in order to speed-up the computation [19, 20]. The limited numerical aperture of our objective (NA=0.3) prevents the light scattered at an angle larger than arcsin(NA) to be observed. Reducing the scattering angle cone corresponds to the operation of filtering out from the complex scattered field the spatial frequencies above NA/λ [21, 22]. In the fitting routine, when computing $\mathbf{f}$, we take into account this effect by filtering out frequency components larger than the cutoff value. This cutoff frequency is obtained by a preliminary fitting on a set of holograms of a polystyrene bead at ambient pressure. The obtained cutoff value corresponds to an effective numerical aperture of 0.285 and is kept fixed in all subsequent fitting procedures.

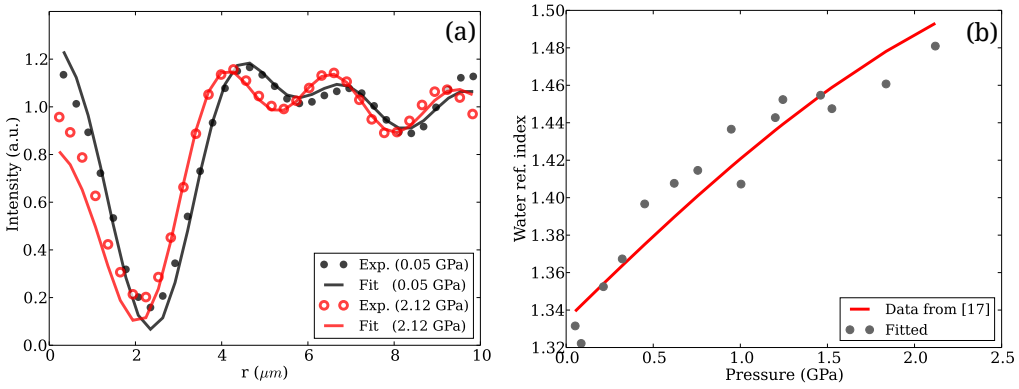

Fig. 2. (a) Radial averages of experimental holograms at low (gray dots) and high (red dots) pressures. The corresponding fitting curves are plotted respectively by gray and red lines. (b) Water refractive index as function of pressure. Gray dots plot the values obtained from the holograms leaving n_w as a fit parameter. The red line plots previously reported data [18].

Since the sample is observed through a L_{dia}=1.55 mm thick diamond window, both the incident and the scattered fields will propagate through a thick slab with a refractive index of $n_{dia} = 2.4$ that introduces aberrations. These aberrations can be taken into account by considering $\mathbf{f}$ as a sum of plane waves. Each of these plane waves will acquire a phase shift $L_{dia}(k_z^{dia} - k_z^{air})$, where k_z^{dia} and k_z^{air} are the wavevector components along the optical axis z respectively in diamond and in air. The 2D Fourier transform of $\mathbf{f}$, with transverse wavevector (k_x, k_y), corresponds to a plane wave with $k_z = [(2\pi n/\lambda)^2 - k_x^2 - k_y^2]^{1/2}$. The aberration can be then computed by multiplying the Fourier transform of $\mathbf{f}$ by:

$$\exp\left[i\left(\sqrt{\left(\frac{2\pi n_{dia}}{\lambda}\right)^2 - k_x^2 - k_y^2} - \sqrt{\left(\frac{2\pi n_{air}}{\lambda}\right)^2 - k_x^2 - k_y^2}\right) L_{dia}\right]$$

and then by transforming back.

Inset in Fig. 1(b) shows a typical hologram of a 5 μm polystyrene bead trapped inside the

Optics EXPRESS

DAC chamber. The trap has been displaced by the SLM 40 μm above the focal plane so that the fringes due to the interference between scattered and incident light are well visible. Other non trapped beads sediment on the bottom diamond surface that is closer to the focal plane so that the corresponding fringe patterns have a reduced lateral extent. To avoid interference with these other particles we only fitted interference pattern within the region delimited by the black dashed line. The black line in Fig. 1(b) plots the radial profile, averaged over the azimuthal coordinate, of the experimental fringes in the hologram. The red line in Fig. 1(b) represents the curve corresponding to the best fitting hologram computed as in Eq. 1. To highlight the importance of including the effects given by the limited numerical aperture and the aberration due to the diamond window, we plot as a red dashed line the curve that one obtains with the same bead parameters and without including the aforementioned corrections. To have a better insight of our method, we show in Fig. 2(a) the radial average of two holograms at low (0.05 GPa) and high (2.12 GPa) pressure and their corresponding fits. Our procedure is able to fit the experimental data giving us the bead parameters at different pressures.

Pressure in the DAC chamber is monitored by measuring the fluorescent emission of a 20 μm ruby bead placed in the sample. To excite the fluorescence, we use a green laser diode (λ = 532 nm) focused on the ruby by the microscope objective, while the emitted light is collected by an optical fiber and sent to a spectrometer (Ocean Optics HR4000). As pressure increases the ruby fluorescence spectrum peaks shift towards longer wavelengths [23] (see Fig. 1(a)). The pressure is obtained by comparing the observed emission peaks' wavelengths with the calibration data given in [24].

3. Results

The DAC chamber has been loaded with 5 μm polystyrene beads (Bangs Laboratories) dispersed in deionized water. A small quantity of surfactant (2% 140000 Extran MA5) has been used to reduce adhesion of beads to the diamonds' facets. We trapped a single polystyrene bead and recorded its Brownian fluctuations for 60 s at 1 KHz framerate. We acquired data for 15 different pressures ranging from ambient pressure to 2.1 GPa. At ambient temperature, water crystallization occurs at 1 GPa meaning that we acquired data also when water is in a metastable state. Any pressure change on the controller was followed by 30 minutes waiting time to reach the equilibrium stationary state. After data acquisition we analyze the holograms and, as explained in the previous section, we extract the particle trajectory and the particle radius a. From the in-plane motion of the trapped bead we extract the fluctuations power spectrum that has the form [25]:

$$PSD(\omega) = \frac{\mu k_B T}{\pi} \frac{1}{\omega^2 + (\mu k)^2} \tag{2}$$

where k_B is the Boltzmann constant, T is the absolute temperature, k is the trap elastic constant, and μ is the particle mobility. By fitting the measured power spectrum with Eq. 2 we extract both the values of k and μ whose relative uncertainties, which are estimated from the covariance matrix of the fit parameters, are respectively 1.5% and 1%. When the bead is sufficiently far away from confining walls the mobility is given by Stokes formula $\mu = 1/(6\pi\eta a)$ with a bead's radius and η solvent viscosity. Although we can extract the mobility with good precision from PSD fits, an accurate determination of viscosity requires an equally accurate knowledge of the bead radius a. In our previous study [12], we tracked beads using bright field microscopy which does not allow to determine the bead radius with an accuracy that is better then the nominal values provided by the manufacturer $a = 5.0 \pm 0.5$ μm. Conversely, here through DHM tracking of a bead inside a DAC we demonstrate direct and accurate determination of bead size for all investigated pressures.

In order to highlight the importance of a direct bead sizing we report as gray circles in Fig. 3(a) the viscosities obtained using a fixed value for the bead radius a, i.e. the measured value

Optics EXPRESS

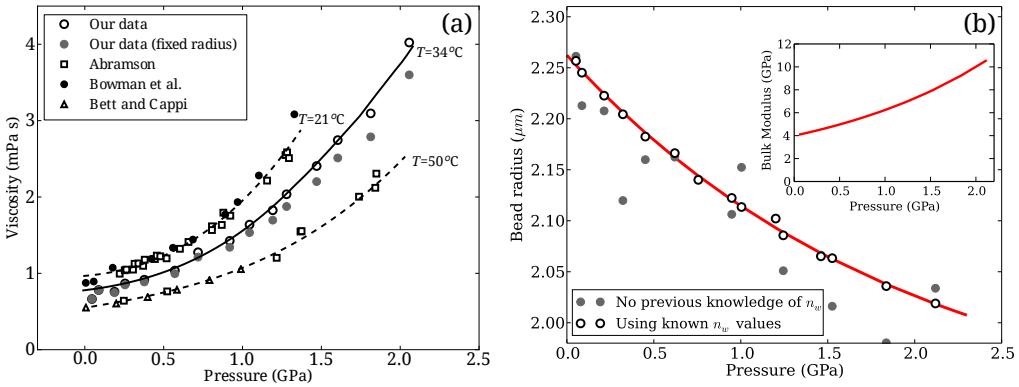

Fig. 3. (a) Water viscosity as a function of pressure. Open circles are obtained using DHM full fits of position and size (solid line is a guide to the eye). Gray circles are obtained using a constant bead size in fits. Squares are Abramson's data [26], triangles are Bett and Cappi's data [27], dotted lines are polynomial fits to Abramson's data. (b) Polystyrene bead radius and bulk modulus (shown in the inset) as functions of pressure. Gray dots are obtained by leaving the water refractive index n_w as a fitting parameter.

at ambient pressure. Empty circles in Fig. 3(a) represent the viscosity values obtained when taking into account bead size variations as obtained from the fitting procedure at each pressure. The relative difference between the two data sets can be quite large (11% for 2.1 GPa). This discrepancy remarks that the knowledge of a is crucial for an accurate measure of viscosity at high pressures. Even when the bead size does not shrink significantly, using the nominal size provided by the manufacturer would cause a systematic error due to the unavoidable polydispersity of the beads [2]. We estimate the precision of our measure of a by computing the standard deviation of the fitting values of a set of holograms, recorded at the same pressure, obtaining a value of 6 nm. Finally we evaluate the precision on η, which is about 2%, by propagating the uncertainties of μ and a.

From the measured η at ambient pressure, we can estimate the temperature inside our sample that, due to absorption of the IR trapping laser [28], could be higher than the room temperature. By interpolating to our temperature value the curve reported in [29] for η as a function of temperature, we get a sample temperature of 34 °C. Empty circles in Fig. 3(b) plot the trapped bead radius as a function of pressure when we leave as fit parameters x_p, y_p, z_p, a, n_p and use the known values of n_w reported in [18]. When n_w is unknown, it can be included among the fitting parameters and thus be measured. However, in that case the precision on fitted values is reduced. Figure 2(b) shows the fitted values of n_w as a function of pressure along with the water refractive index values reported in [18]. Similarly, a decrease in the precision is also manifest in Fig. 3(b) that plots as gray dots the bead radius obtained setting n_w as a fit parameter. Notwithstanding the fact that the points are more scattered, we can still recover the descending trend. A phenomenological curve that follows our data for bead radius as a function of pressure is the following:

$$a(P) = a_* + \Delta a e^{-C(P-P_0)/3}$$

where p_0 is the ambient pressure while a_*, Δa , and C are free parameters. The best fitting curve is plotted as a red solid line in Fig. 3(b). Our phenomenological curve leads to the following isothermal bulk modulus:

Optics EXPRESS

$$K_T(P) = -V\left(\frac{\partial P}{\partial V}\right)_T = -\frac{a(P)}{3}\left(\frac{\partial a(P)}{\partial P}\right)^{-1} = \frac{1}{C}\left(1 + \frac{a_*}{\Delta a}e^{(P-P_0)C/3}\right)$$

The bulk modulus is plotted in the inset in Fig. 3(b) as a function of pressure. Interestingly, in the range we explored, the bulk modulus increases more than a factor of two growing from 4 GPa at ambient pressure, which is in good agreement with previously reported values [30, 31], up to 10 GPa. Once a DAC is available, our technique provides a very convenient and cost effective way of determining bulk moduli of transparent materials that can be produced in colloidal beads, which could be particularly useful in the case of plastic materials. Alternative techniques to access compressibilities at ultra-high-pressures usually involve a much higher degree of complexity and costs in the experimental setup. One way is through direct measurement of atomic structure deformations using X-rays typically from bright and collimated synchrotron sources [32]. Alternatively one can use Brillouin scattering to retrieve the adiabatic bulk modulus from sound speed measurements which requires high contrast spectrometers to detect wavenumber shifts of the order of 1 cm^{-1} [33].

4. Discussion

We have demonstrated that it is possible to perform DHM on a trapped micron-sized bead inside a DAC. This allows to fully 3D track the trapped bead and measure its radius as a function of pressure. DHM is superior to bright field in many respects, and it is simple to extract the information encoded in the experimental holograms when the sample under study is extremely dilute as in the present investigation. In particular, for high pressure physics, the possibility of a precise determination of the size of particles through DHM and Lorenz-Mie scattering theory appears very intriguing. In the present work we used this knowledge to have an accurate measure of water viscosity and to compute the bulk modulus of the polystyrene bead as a function of pressure. Such micron-sized objects, once calibrated, might also be used not only as local rheological probes, but also as local pressure sensors inside the DAC.

Funding

F.S., S.B. and R.D.L. acknowledge funding from the European Research Council under the European Union's Seventh Framework Programme (FP7/2007-2013)/ERC grant agreement no. 307940. R.W.B. acknowledges financial support from Queens' College, Cambridge and the Royal Commission for the Exhibition of 1851.

130.209.115.55 {ts '2016-12-15 09:41:34'}